Title

Increased Striatal Presynaptic Dopamine in a Nonhuman Primate Model of Maternal Immune Activation: A Longitudinal Neurodevelopmental Positron Emission Tomography Study With Implications for Schizophrenia

Journal

Biological Psychiatry Cognitive Neuroscience and Neuroimaging, 8(5)

ISSN

2451-9022

Authors

Smucny, Jason

Vlasova, Roza M

Lesh, Tyler A

et al.

Publication Date

2023-05-01

DOI

10.1016/j.bpsc.2022.10.012

Peer reviewed

HHS Public Access

Author manuscript

Biol Psychiatry Cogn Neurosci Neuroimaging. Author manuscript; available in PMC 2024 May 01.

Published in final edited form as:

Biol Psychiatry Cogn Neurosci Neuroimaging. 2023 May ; 8(5): 505–513. doi:10.1016/j.bpsc.2022.10.012.

Increased Striatal Presynaptic Dopamine in a Nonhuman Primate Model of Maternal Immune Activation: A Longitudinal Neurodevelopmental PET Study with Implications for Schizophrenia

Jason Smucny[1], **Roza M. Vlasova**[2], **Tyler A. Lesh**[1,3], **Douglas J. Rowland**[4], **Guobao Wang**[5], **Abhijit J. Chaudhari**[4,5], **Shuai Chen**[6], **Ana-Maria Iosif**[6], **Casey E. Hogrefe**[7], **Jeffrey L. Bennett**[8], **Cynthia M. Shumann**[1], **Judy A. Van de Water**[9], **Richard J. Maddock**[1], **Martin A. Styner**[2,10], **Daniel H. Geschwind**[11], **A. Kimberley McAllister**[3], **Melissa D. Bauman**[1,7], **Cameron S. Carter**[1,3]

[1]Department of Psychiatry and Behavioral Sciences, University of California, Davis

[2]Department of Psychiatry, University of North Carolina, Chapel Hill

[3]Center for Neuroscience, University of California, Davis

[4]Center for Genomic and Molecular Imaging, University of California, Davis

[5]Department of Radiology, University of California, Davis

[6]Division of Biostatistics, Department of Public Health Sciences, University of California, Davis

[7]California National Primate Research Center

[8]Department of Psychology, University of California, Davis

[9]Rheumatology/Allergy and Clinical Immunology, University of California, Davis

[10]Department of Computer Science, University of North Carolina, Chapel Hill

[11]Department of Neurology, University of California, Los Angeles

Abstract

Background: Epidemiologic studies suggest maternal immune activation (MIA) is a significant risk factor for future neurodevelopmental disorders, including schizophrenia (SZ), in offspring. Consistent with findings in SZ and work in rodent systems, preliminary cross-sectional findings in nonhuman primates suggest MIA is associated with dopaminergic hyperfunction in young adult offspring.

Methods: In this unique, prospective longitudinal study, we used [^{18}F]fluoro-l-m-tyrosine ([^{18}F]FMT) PET to examine the developmental time course of striatal presynaptic dopamine synthesis in male rhesus monkeys born to dams (n=13) injected with a modified form of the

Correspondence: Jason Smucny, Ph.D., jsmucny@ucdavis.edu; Cameron S. Carter, M.D., cscarter@ucdavis.edu.

Disclosures

The authors declare no competing financial interests.

inflammatory viral mimic, Polyinosinic:polycytidylic acid, in the late first trimester. Striatal (caudate, putamen, and nucleus accumbens) dopamine was compared to control offspring born to dams that received saline (n=10) or no injection (n=4). Dopamine was measured at 15, 26, 38, and 48 months of age. Prior work from this cohort found decreased prefrontal gray matter volume in MIA offspring vs. controls between 6–45 months of age. Based on theories of the etiology and development of SZ-related pathology, we hypothesized a delayed (relative to the gray matter decrease) increase in striatal FMT signal in the MIA group vs. controls.

Results: [^{18}F]FMT signal showed developmental increases in both groups in the caudate and putamen. Group comparisons revealed significantly greater caudate dopaminergic signal in the MIA group at 26 months.

Conclusions: These findings are highly relevant for the known pathophysiology of SZ and highlight the translational relevance of the MIA model in understanding mechanisms by which MIA during pregnancy increases risk for later illness in offspring.

Keywords

Caudate; Dopaminergic; Inflammation; Macaque; Putamen; Striatum

Introduction

Neuroimmune perturbations early in development are now recognized as significant risk factors for future mental health problems. Indeed, a multitude of epidemiologic evidence suggests that infections during pregnancy increase the likelihood that offspring will develop illnesses such as schizophrenia (SZ) and bipolar disorder with psychotic features (1–9). This increased risk is mediated by the maternal immune response (in addition to biologically damaging direct effects of the pathogenic agent) (10–12). Understanding the mechanisms by which maternal immune activation (MIA) may alter neurodevelopment and the function of key neural systems associated with risk for neurodevelopmental and mental health disorders is therefore of paramount importance, especially considering the current COVID-19 pandemic (13).

Animal MIA model systems have provided important insights regarding the behavioral, systems and cellular and molecular mechanisms changes resulting from MIA (14, 15). Using these models, researchers have found that offspring of mothers who experience MIA show neurodevelopmental abnormalities, including striatal dopaminergic hyperfunction, that may be related to various mental disorders such as SZ (16–18). This critical data from the rodent model provides a strong premise for determining if the association between MIA and hyperdopaminergia is present in a species more physiologically, developmentally, and behaviorally related to humans, such as the nonhuman primate (NHP) rhesus macaque (*Macaca mulatta)* (19, 20).

To that end, over the past several years we at the University of California, Davis Conte Center have examined the effects of a modified form of the MIA agent Polyinosinic:polycytidylic acid (Poly IC, stabilized with polylysine and carboxymethylcellulose; also known as Hiltonol®), a viral mimic, on NHP offspring

neuroanatomy, physiology, and behavior (21). Pilot work from a small cohort of male monkeys (n=5 first trimester + n=4 second trimester MIA-exposed vs. 4 saline-exposed or unexposed controls) found that in addition to a transient maternal immune response, Poly IC induced increased repetitive behaviors and abnormal social behaviors in offspring (22–24). We also performed PET imaging using the presynaptic dopamine tracer [^{18}F] fluoro-l-m-tyrosine (FMT) at 3.5 years of age in these macaques. Consistent with murine MIA models (25, 26), we found preliminary evidence for presynaptic striatal hyperdopaminergia in the MIA group (27). These findings are consistent with the neurochemistry of SZ, for which elevated striatal presynaptic dopamine has been repeatedly observed (28–35).

Although these early findings were encouraging in that they were consistent with the highly replicable hyperdopaminergic phenotype of SZ, the developmental time course of this divergence remains unclear. Indeed, SZ is increasingly being recognized as a neurodevelopmental disorder (36, 37), based on evidence that cognitive deficits may be evident as early as childhood in people who later developed SZ-spectrum disorders (38, 39). Prominent theories of the etiology of SZ posit that the initial developmental pathophysiology occurs in the dorsolateral prefrontal cortex (DLPFC), which plays a prominent role in regulating the activity of midbrain dopaminergic nuclei. Specifically, it is posited that an initial loss of dopaminergic input from the brainstem to the DLPFC leads to subsequent downstream changes (e.g., hyperdopaminergia) in subcortical regions such as the striatum as a compensatory response (40, 41). According to this framework, one would hypothesize to observe prefrontal pathology in SZ months in years prior to the increase in striatal presynaptic dopamine. Accordingly, we have previously published longitudinal findings demonstrating a loss of prefrontal volume starting at 6 months and persisting through 45 months of age in MIA-treated animals (42). Here, in this new, larger (compared to our pilot study (27)) cohort of Poly IC and control animals, we report on longitudinal changes in presynaptic dopamine as assessed by [^{18}F]FMT PET, providing a unique test of the neurodevelopmental hypothesis in a system with neurodevelopmental perturbation due to a known risk factor for SZ (e.g., MIA). Based on the neurodevelopmental hypothesis described above and our preliminary data, we hypothesized striatal hyperdopaminergia in these animals starting at a later timepoint and then persisting through the 48-month assessment.

Methods and Materials

Overview

Structural neuroimaging and cognitive data of the cohort in the present study has been previously published (42). All experimental procedures were developed in collaboration with the veterinary, animal husbandry, and environmental enrichment staff at the California National Primate Research Center (CNPRC) and approved by the University of California, Davis Institutional Animal Care and Use Committee. All attempts were made to promote species-typical social development and psychological well-being of the animals that participated in this research (in terms of social housing, enriched diet, use of positive reinforcement strategies, and minimizing the duration of daily training/testing sessions). Gestational timing, choice of species, source of immune activating agent, and subsequent

magnitude of the MIA response determine the impact on offspring neurodevelopment in preclinical MIA models. In accordance with recent guideline recommendations for improving the reporting of MIA model methods, we have filled out the template from (43) and provided it as Table S1.

Animal Selection

Pregnant dams were selected from the indoor, time-mated breeding colony based on age, weight, parity, and number of prior live births. Dam characteristics (age at conception, weight, and prior conceptions) are provided in (42)). Candidate dams between 5 and 12 years old carrying a male fetus were assigned to MIA (n=14) and control/saline (n=10). Due to limited availability of male fetuses, unexposed pregnant females confirmed to be carrying male fetuses were added to the control group (n=4). One offspring from the MIA group was euthanized at 6 months of age due to an unrelated health condition and is not included in this report. A second animal from the MIA-exposed group was euthanized at 42 months of age also due to an unrelated health condition.

Maternal Immune Activation and Validation

MIA induction protocols were based on our previous dosing and gestational timing experiments (22, 23, 27, 42, 44, 45). Synthetic double-stranded RNA (Poly IC stabilized with poly-L-lysine (Oncovir, Inc.; 0.25 mg/kg i.v.) or sterile saline (equivalent volume to Poly IC) was injected at 07:30 hours in the cephalic vein in awake animals on gestational day (GD) 43, 44, and 46 (see (42) for detailed protocol). Health and behavior observations were conducted three times pre-exposure, 6 hours after each of the three injections, and three times post-exposure. The checklist captured the presence or absence of any clinical or behavioral symptoms resulting from the infusions including change in appetite, watery eyes or nasal discharge, liquid stool, lethargy or labored movements, and body temperature. Prior to infusions, programmable temperature microchips (Bio Medic Temperature Systems, Seaford, DE) were implanted subcutaneously under sedation near the left and right clavicle, and a temperature wand then scanned the microchip and displayed body temperature. Temperatures were recorded just prior to Poly IC or saline injection, and 30 minutes, 6 hours, and 8 hours after injection. Pre- and post-exposure baseline temperatures were taken during health and behavior observations. Blood was collected from the dams on approximately GD 40 while sedated for ultrasound (pre-exposure), from awake animals on GD 44 and 46, 6 hours after Poly IC infusion, and on GD 51 or 52 while sedated for a recheck ultrasound (post-exposure) for cytokine analysis. Blood samples were centrifuged, and the serum was removed, aliquoted into 200 uL samples, and frozen at −80°C until analysis. A longitudinal examination on the maternal IL-6 response to Poly IC exposure was measured in serum using a NHP multiplexing bead immunoassay (MilliporeSigma, Burlington, MA) that was analyzed using the flow-based Luminex™ 100 suspension array system (Bio-Plex 200; Bio-Rad Laboratories, Inc.).

Rearing Conditions and Husbandry

Infants were raised in individual cages with their mothers where they always had visual access to other mother-infant pairs. Additional significant socialization procedures were also applied (see Supplementary Material for details re: socialization, rearing, and husbandry).

Structural Neuroimaging

To generate regions of interest (ROIs) for PET analysis, structural magnetic resonance imaging of the brain was performed when the monkeys were approximately 12, 24, 36, and 45 months of age using a Siemens Magnetom Skyra 3-T (Siemens Medical Solutions, Erlangen, Germany) with an 8-channel receiver coil optimized for monkey brain scanning (Rapid MRI, Columbus, Ohio). It was determined that two of the animals (one in the MIA group and one in the control group) were sensitive to isoflurane, therefore, at subsequent timepoints, these animals were scanned using propofol as the anesthetic[1].

The rate of infusion varied to maintain the animal at a steady state of anesthesia. All other animals at all timepoints were sedated with ketamine for tracheal intubation, then anesthetized with isoflurane for positioning in an MR-compatible stereotaxic apparatus. Once the animal was placed in and centered at the mid-line of the stereotaxic apparatus, the 8-channel receiver coil was attached to the stereotaxic apparatus using a custom connector. Anesthesia was maintained with isoflurane at 1.3–2.0%. Fluids were maintained with a saline infusion at a rate of 10 mL/kg/hr for the duration of the MRI scan.

T_1-weighted images (480 sagittal slices) were acquired with TR=2500 ms, TE=3.65 ms, flip angle=7°, field of view 256 × 256, voxel size during acquisition 0.6 × 0.6 × 0.6 mm. Acquired images were interpolated during image reconstruction to 512 × 512 voxels with a final resolution voxel size of 0.3 × 0.3 × 0.3 mm.

Regions-of-Interest

T_1-weighted images were segmented into gray matter, white matter, and cerebrospinal fluid using NeosegPipeline_v1.0.8 (46). The gray matter of the cerebellum and bilateral subcortical regions of interest (ROIs; caudate, putamen, and nucleus accumbens (NAcc)) were segmented using a multi-atlas segmentation in AutoSeg_3.3.2 (47) with publicly available atlases (www.nitrc.org/projects/unc_macaque/).

Positron Emission Tomography

The [^{18}F]FMT synthesis and animal preparation followed our previously reported protocol (27). [^{18}F]FMT behaves similarly to [^{18}F]FDOPA and is metabolized in the periphery, causing lower bio-availability in the brain (48). To avoid this metabolism, 5 mg/kg carbidopa was administered as a peripheral decarboxylase inhibitor (48–52) approximately 45 min prior to injection of [^{18}F]FMT. The cephalic vein was used for carbidopa and radiotracer injection. For PET imaging, the anesthetized (with isoflurane or propofol (n = 2); see Structural Neuroimaging, above) monkey was placed on a custom-built bed, head-first, into the bore of the PiPET scanner (Brain Biosciences, Rockville, MD 20852, spatial resolution ~2.0 mm). A cold transmission scan was acquired followed by [^{18}F]FMT injection (~18.5 MBq/kg). A 90-min dynamic emission PET scan was conducted starting approximately 10 s prior to injection of [^{18}F]FMT. Data were reconstructed using the maximum likelihood expectation maximization method into 24 frames of the following durations: 10 frames at 1

[1]In our prior neuroanatomical paper[42] we stated that three animals were sensitive to isoflurane. By 12 months, one of these animals passed a tolerance test and thus was switched back to isoflurane, explaining the discrepancy.

min each, 5 frames at 2 min each, 4 frames at 5 min each, and 5 frames at 10 min each. Images were acquired when the monkeys were approximately 15, 26, 38, and 48 months of age.

PET data were analyzed using PMOD v. 3.9 software (PMOD Technologies Ltd, Zurich, Switzerland). First, individual PET time series images were summed and registered to skull-stripped anatomical images of each animal using the PMOD automated registration function. Registrations were subsequently visually inspected for accuracy. The calculated registration matrix was then applied to the dynamic, unsmoothed PET data. Consistent with our prior work (27), index of influx (K_i) [^{18}F]FMT values for each ROI were determined using the Patlak reference tissue model with the cerebellum as a reference region and a time cutoff value of 25 min for model fitting (53, 54). K_i values were normalized by V_0, the volume of distribution in the reversible compartment (estimated as the Patlak intercept), to provide the [^{18}F]FMT influx rate per unit [^{18}F]FMT distribution volume (55, 56). K_i/V_0 values were considered indices of the concentration of bound [^{18}F]FMT relative to the concentration of free [^{18}F]FMT and thus presynaptic dopamine.

Statistical Analysis

Linear mixed-effects models (57) were used to model presynaptic dopamine synthesis capacity trajectories and to evaluate group differences between 15 and 48 months of age. This approach explicitly accounts for multiple measurements per animal and allows for unequally spaced and missing observations. Separate linear mixed-effects models were built to examine the trajectories of K_i/V_0 for each brain region (caudate, putamen, and NAcc). Initial evaluations focused on determining the optimal covariance structure to account for within-subject dependence due to the repeated measures, assessing model fit using Akaike information criteria (AIC). As described in detail in the Supplement, several candidate covariance structures were considered for each brain region. All initial models were full models, i.e., included group (MIA vs. control), linear, quadratic, and cubic effects of age at scan (measured in months, centered at 15 months) and interactions between the linear, quadratic, and cubic age effects and group. The interaction terms between group and the linear, quadratic, and cubic effects of age allowed for differences between groups in the linear, quadratic, and cubic trajectories, respectively. The final covariance structure chosen by AIC was spatial exponential for the putamen and NAcc. For caudate, the best within-animal covariance was modeled by including a random intercept and random slope for age (see the Supplement for more technical details). Once the covariance structure was selected, further model development was carried out. For each region, interaction effects and quadratic and cubic age effects were trimmed by sequentially removing those with p values > 0.05. Candidate models including a given interaction or higher order age effect retained all corresponding lower-order terms. Significant group by age interactions in the final models were followed up by planned comparisons between groups to determine which, if any, [^{18}F]FMT PET signals were significantly different at each of the four scanning timepoints. At each timepoint, effect sizes were calculated using Cohen's D = (MIA mean-Control mean)/SD (58) where the group differences (MIA mean-Control mean) were estimated based on the fitted mixed-effects models, and SDs were the pooled standard deviations from MIA and control group at that timepoint.

To further assess the strength of the evidence for group differences at each timepoint, Bayes factors were approximated by exponentiating (BIC_{null} - $BIC_{alternative}$)/2, where BIC_{null} is the Bayesian information criterion (BIC) under the null model (i.e., group difference is 0 at a specific timepoint) and $BIC_{alternative}$ is the BIC under the alternative model (i.e., the final model) (59). The Supplement includes the equations for the null and alternative models. Bayes factors between 3 – 10, 10 – 30, and > 30 were interpreted as moderate, strong, and very strong/extreme evidence for the alternative hypothesis, respectively; between 1/3 – 1/10, 1/10 – 1/30, and < 1/30 were interpreted as moderate, strong, and very strong/extreme evidence for the null, respectively. A Bayes factor between 1/3 and 3 suggested only weak or "anecdotal" evidence (59).

Finally, to evaluate the effects of different anesthetics (isoflurane vs. propofol), a sensitivity analysis was performed by excluding the two animals that were given propofol and re-fitting the final models.

Analyses were conducted using SAS v. 9.4 (SAS Institute Inc., Cary, NC). All tests were two-sided, and *p*-values < .05 were considered statistically significant. Additional technical details of the statistical analyses are provided in the Supplement.

Results

Maternal Inflammatory Response

As described previously (42), MIA induced an inflammatory response as indexed by an elevation of interleukin-6 levels in plasma from baseline at 6 hours following Poly IC injection as well as sickness behaviors (reduced appetite, fever) in dams.

PET Analysis

Age, weight, dose, and [^{18}F]FMT PET signal summary data for each timepoint are provided in Table 1. A representative PET scan from a macaque in the MIA group taken at 26 months with outlined ROIs is shown in Figure 1. Individual [^{18}F]FMT PET signals trajectories over time for the caudate, putamen, and NAcc are shown in Figure 2. The results of the mixed-effects analysis are presented in Table 2.

Significant linear, squared, and/or cubic effects of age were observed for K_i/V_0 in the three regions (Table 2), as K_i/V_0 increased over time in the caudate and putamen across the MIA and control groups. Significant linear and quadratic age by group interactions were also observed in the caudate and putamen, indicating the MIA group had significantly different linear and curvilinear trajectories than the control group (Table 2). Linear contrasts evaluating group differences at each timepoint revealed that K_i/V_0 values were significantly different between groups in the caudate at 26 months of age (Table 2), with greater dopamine synthesis capacity in the MIA-exposed group. The pattern in the putamen and NAcc was similar (with dopamine synthesis capacity qualitatively higher at 26 months for the MIA group in general) but these differences did not reach statistical significance.

Bayes factor analysis also demonstrated strong evidence for a group difference at 26 months in the caudate with only weak support for differences at other timepoints or regions (Table

2). A sensitivity analysis excluding the two animals anesthetized with propofol yielded similar estimated model coefficients and findings as the primary analysis (Table S2).

Discussion

In this unique, longitudinal PET neuroimaging study, we examined levels of striatal presynaptic dopamine across childhood and adolescence in a NHP model of MIA. Consistent with previous neurodevelopmental studies in NHPs (60, 61), dorsal striatal presynaptic dopamine levels increased (linearly and/or curvilinearly) across all groups from the 15-month baseline to 48 months of age. Furthermore, in agreement with our hypothesis, a significant interaction between group and age was also observed on presynaptic dopamine levels. This interaction resulted in group difference at 26 months of age and, interestingly, normalized by 38 months of age. Bayes factor analysis, furthermore, confirmed strong evidence for a group difference at 26 months of age but no evidence for group differences at any other timepoint.

Our finding of increased striatal presynaptic dopamine in MIA-exposed animals highlights the unique translational significance of this animal model system as it manifests a core phenotype that is uniquely relevant to psychotic disorders, specifically SZ (28–35). It also suggests a possible neurochemical link between inflammation during pregnancy and greater risk for future mental illness in offspring. Although elevated presynaptic dopamine is now well-established in SZ, to this point studies have not yet determined when this increase occurs during development, as PET imaging studies require injection of radioactive elements unsuitable for use in children. Hence, elucidating the full developmental time course of striatal hyperdopaminergia in at risk populations benefits greatly from the use of translational animal model systems such as NHPs. The results of this study suggest that MIA, which is a known risk factor for SZ, induces a striatal hyperdopaminergic state as early as 26 months of age in NHPs. In male rhesus monkeys, pubertal onset generally occurs between 3–4 years of age (62, 63); thus, while establishing age equivalence for NHPs and humans is imprecise, the transient elevation in striatal dopamine seen in the present study occurred during a period of development roughly equivalent to late childhood in humans. Future studies using emerging technologies such as low-dose, high sensitivity PET (64) or nonradioactive magnetic resonance imaging-based neuromelanin quantification (a dopamine proxy marker) (65) may help determine if similar increases in dopamine occur in at risk humans during this period of development.

Notably, our analysis of brain structure in this cohort found subtle and selective cognitive deficits (affecting measures of attention and cognitive flexibility) emerging around 2 years of age, along with reduced gray matter volume loss in the prefrontal cortex present at 6 months of age and persisting throughout the 4-year follow-up period. In conjunction with these longitudinal behavioral and structural MRI findings, the present study provides us with a unique test of a prominent neurodevelopmental model of dopaminergic dysregulation in psychosis – namely that pathophysiological changes in the prefrontal cortex precede dopamine dysregulation due to a loss of prefrontal inhibition via projections to the SN/VTA. Our results in this NHP MIA cohort align with predictions of this model, with early structural pathology in the PFC preceding the development of dopamine dysregulation by

18 months or the equivalent of roughly 6 human years (40, 41). Our finding of significant increases in FMT signal in the MIA group vs. controls in the caudate but not ventral striatum is also in agreement with meta-analytic evidence suggesting the most robust differences in presynaptic dopamine are in the dorsal (associative) striatum (66). Although the mechanism is unclear, one possibility is that changes in the function of the prefrontal cortex, reflected by a loss of gray matter volume early in development, leads to a reduction in glutamatergic input to the SN/VTA and (over time) dysregulation of dopaminergic neuronal activity (67). Supporting this view, studies suggest the striatal region with the most DLPFC input – namely, the dorsal striatum – is the region that shows the highest increase in dopaminergic tone in SZ (66). Recent work also suggests that in patients with SZ that respond to antipsychotics, prefrontal volumes are inversely correlated with elevated striatal dopamine (68). To more closely examine DLPFC structure and function in the MIA model and their relationships with dopamine, future planned studies by our group include postmortem analysis of DLPFC spine number and morphology as well as measures of local circuity integrity (including cellular and subcellular characterization of inhibitory interneurons) as has been extensively conducted in SZ (69). Of note, a preliminary analysis using the Golgi method in an early, adolescent pilot MIA NHP cohort showed alterations in dendritic morphology in layer III pyramidal cells of the DLPFC (45).

In our previous pilot study, we reported increased dopamine in a smaller cohort of 3.5-year-old macaques born to dams who experienced Poly IC-induced MIA in the first or second trimester (27). Interestingly, the dopamine increase observed in the MIA cohort described here was transient, occurring at 26 months of age but not at later timepoints. This intriguing finding suggests that this increase may be reversible. What may be the reasons why this reversal occurred? One possible account of this variability across the two cohorts is that it may reflect differences in animal housing and activities between the two studies. For example, animals in the present study were permanently paired with a home cage partner throughout the study duration (monkeys in the first study were only paired starting between 18–24 months of age), and socialization can moderate stress responses (70–73) and reduce the likelihood of transition to psychosis from high risk status (74–77). Additionally, restraint during an eye tracking task in the prior study was not used here, suggesting that the additional stress in the first group may have exacerbated MIA effects (78, 79). Finally, animals in the present study underwent daily cognitive exercises, which may have helped to partially remediate PFC dysfunction (80) and provide better modulation of subcortical systems (including the ventral tegmental area) where dopamine-producing neurons are located (81). It is also possible that if we had followed the animals in the present study for a longer period, we might have seen further evidence of behavioral and dopaminergic system dysregulation as the animals progressed into adulthood. It should also be noted that the previous pilot study used a very small sample size (n=9 MIA animals and 4 controls) and we cannot rule out that the previous result may have been a false positive. We also cannot rule out the possibility that group differences in FMT biotracer availability affected the observed results. Nonetheless, while speculative, an exciting possibility is that striatal hyperdopaminergia may ameliorate in socially and/or cognitively enriched environments. Indeed, such a neurodevelopmental perspective is consistent with the idea

that MIA exposures very early in development (i.e., years before illness onset) may be preventative and thus confer the most clinical benefit (36).

Taken together with the effects of MIA-exposure on cognition and structural brain development reported previously (42), these results suggest that MIA during the first trimester of pregnancy is associated with the development of a behavioral and neural systems phenotype that is highly relevant for understanding the developmental pathophysiology of SZ. Notable limitations of the study were the small sample size and potential confounding effects of cognitive training and socialization as well as potential group differences in FMT tracer bioavailability and response to anesthetics. Future studies based upon this MIA NHP cohort, including cellular and molecular analyses of the atypically developing circuitry identified in this and our previous report, will provide additional insights into the pathophysiological mechanisms by which maternal infections may increase risk for serious mental illness in humans.

Supplementary Material

Refer to Web version on PubMed Central for supplementary material.

Acknowledgements

Funding for the study was provided by National Institutes of Mental Health grant P50 MH106438. PET imaging was performed with instrumentation provided by National Institutes of Health grant S10 OD021715. Poly IC was kindly provided by Dr. Andres Salazar, MD, Oncovir, Washington D.C. Development of the nonhuman primate model and behavioral characterization of the offspring were supported by P50 MH106438-6618 to MDB. Neuroimaging studies were supported by P50 MH106438-6617 to CSC. Cytokine analysis was supported by the Biological and Molecular Analysis Core of the Medical Investigation of Neurodevelopmental Disorders Institute Intellectual and Developmental Disabilities Research Center (P50 HD103526). Additional support was provided by the base grant (RR00169) of the CNPRC. We thank the veterinary and animal services staff of the CNPRC for care of the animals.

References

1. Estes ML, McAllister AK (2016): Maternal immune activation: Implications for neuropsychiatric disorders. Science. 353:772–777. [PubMed: 27540164]
2. Kepinska AP, Iyegbe CO, Vernon AC, Yolken R, Murray RM, Pollak TA (2020): Schizophrenia and Influenza at the Centenary of the 1918–1919 Spanish Influenza Pandemic: Mechanisms of Psychosis Risk. Front Psychiatry. 11:72. [PubMed: 32174851]
3. Allswede DM, Buka SL, Yolken RH, Torrey EF, Cannon TD (2016): Elevated maternal cytokine levels at birth and risk for psychosis in adult offspring. Schizophr Res. 172:41–45. [PubMed: 26897476]
4. Avramopoulos D, Pearce BD, McGrath J, Wolyniec P, Wang R, Eckart N, et al. (2015): Infection and inflammation in schizophrenia and bipolar disorder: a genome wide study for interactions with genetic variation. PLoS One. 10:e0116696. [PubMed: 25781172]
5. Borglum AD, Demontis D, Grove J, Pallesen J, Hollegaard MV, Pedersen CB, et al. (2014): Genome-wide study of association and interaction with maternal cytomegalovirus infection suggests new schizophrenia loci. Mol Psychiatry. 19:325–333. [PubMed: 23358160]
6. Brown AS, Schaefer CA, Quesenberry CP Jr., Liu L, Babulas VP, Susser ES (2005): Maternal exposure to toxoplasmosis and risk of schizophrenia in adult offspring. Am J Psychiatry. 162:767–773. [PubMed: 15800151]
7. Canetta S, Sourander A, Surcel HM, Hinkka-Yli-Salomaki S, Leiviska J, Kellendonk C, et al. (2014): Elevated maternal C-reactive protein and increased risk of schizophrenia in a national birth cohort. Am J Psychiatry. 171:960–968. [PubMed: 24969261]

8. Severance EG, Gressitt KL, Buka SL, Cannon TD, Yolken RH (2014): Maternal complement C1q and increased odds for psychosis in adult offspring. Schizophr Res. 159:14–19. [PubMed: 25195065]
9. Canetta SE, Bao Y, Co MD, Ennis FA, Cruz J, Terajima M, et al. (2014): Serological documentation of maternal influenza exposure and bipolar disorder in adult offspring. Am J Psychiatry. 171:557–563. [PubMed: 24480930]
10. Han VX, Patel S, Jones HF, Dale RC (2021): Maternal immune activation and neuroinflammation in human neurodevelopmental disorders. Nat Rev Neurol. 17:564–579. [PubMed: 34341569]
11. Han VX, Patel S, Jones HF, Nielsen TC, Mohammad SS, Hofer MJ, et al. (2021): Maternal acute and chronic inflammation in pregnancy is associated with common neurodevelopmental disorders: a systematic review. Transl Psychiatry. 11:71. [PubMed: 33479207]
12. Meyer U (2019): Neurodevelopmental Resilience and Susceptibility to Maternal Immune Activation. Trends Neurosci. 42:793–806. [PubMed: 31493924]
13. Foo SS, Cambou MC, Mok T, Fajardo VM, Jung KL, Fuller T, et al. (2021): The systemic inflammatory landscape of COVID-19 in pregnancy: Extensive serum proteomic profiling of mother-infant dyads with in utero SARS-CoV-2. Cell Rep Med. 2:100453. [PubMed: 34723226]
14. Bergdolt L, Dunaevsky A (2019): Brain changes in a maternal immune activation model of neurodevelopmental brain disorders. Progress in neurobiology. 175:1–19. [PubMed: 30590095]
15. Brown AS, Meyer U (2018): Maternal Immune Activation and Neuropsychiatric Illness: A Translational Research Perspective. Am J Psychiatry. 175:1073–1083. [PubMed: 30220221]
16. Meyer U, Feldon J (2010): Epidemiology-driven neurodevelopmental animal models of schizophrenia. Progress in neurobiology. 90:285–326. [PubMed: 19857543]
17. Ozawa K, Hashimoto K, Kishimoto T, Shimizu E, Ishikura H, Iyo M (2006): Immune activation during pregnancy in mice leads to dopaminergic hyperfunction and cognitive impairment in the offspring: a neurodevelopmental animal model of schizophrenia. Biological psychiatry. 59:546–554. [PubMed: 16256957]
18. Zuckerman L, Rehavi M, Nachman R, Weiner I (2003): Immune activation during pregnancy in rats leads to a postpubertal emergence of disrupted latent inhibition, dopaminergic hyperfunction, and altered limbic morphology in the offspring: a novel neurodevelopmental model of schizophrenia. Neuropsychopharmacology. 28:1778–1789. [PubMed: 12865897]
19. Bauman MD, Schumann CM (2018): Advances in nonhuman primate models of autism: Integrating neuroscience and behavior. Exp Neurol. 299:252–265. [PubMed: 28774750]
20. Testard C, Tremblay S, Platt M (2021): From the field to the lab and back: neuroethology of primate social behavior. Curr Opin Neurobiol. 68:76–83. [PubMed: 33567386]
21. Ryan AM, Bauman MD (2022): Primate models as a translational tool for understanding prenatal origins of neurodevelopmental disorders associated with maternal infection. Biol Psychiatry Cogn Neurosci Neuroimaging.
22. Bauman MD, Iosif AM, Smith SE, Bregere C, Amaral DG, Patterson PH (2014): Activation of the maternal immune system during pregnancy alters behavioral development of rhesus monkey offspring. Biological psychiatry. 75:332–341. [PubMed: 24011823]
23. Machado CJ, Whitaker AM, Smith SE, Patterson PH, Bauman MD (2015): Maternal immune activation in nonhuman primates alters social attention in juvenile offspring. Biological psychiatry. 77:823–832. [PubMed: 25442006]
24. Rose DR, Careaga M, Van de Water J, McAllister K, Bauman MD, Ashwood P (2017): Long-term altered immune responses following fetal priming in a non-human primate model of maternal immune activation. Brain, behavior, and immunity. 63:60–70. [PubMed: 27876552]
25. Eyles D, Feldon J, Meyer U (2012): Schizophrenia: do all roads lead to dopamine or is this where they start? Evidence from two epidemiologically informed developmental rodent models. Transl Psychiatry. 2:e81. [PubMed: 22832818]
26. Meyer U, Feldon J (2009): Prenatal exposure to infection: a primary mechanism for abnormal dopaminergic development in schizophrenia. Psychopharmacology (Berl). 206:587–602. [PubMed: 19277608]

27. Bauman MD, Lesh TA, Rowland DJ, Schumann CM, Smucny J, Kukis DL, et al. (2019): Preliminary evidence of increased striatal dopamine in a nonhuman primate model of maternal immune activation. Transl Psychiatry. 9:135. [PubMed: 30979867]
28. Reith J, Benkelfat C, Sherwin A, Yasuhara Y, Kuwabara H, Andermann F, et al. (1994): Elevated dopa decarboxylase activity in living brain of patients with psychosis. Proc Natl Acad Sci U S A. 91:11651–11654. [PubMed: 7972118]
29. Nozaki S, Kato M, Takano H, Ito H, Takahashi H, Arakawa R, et al. (2009): Regional dopamine synthesis in patients with schizophrenia using L-[beta-11C]DOPA PET. Schizophr Res. 108:78–84. [PubMed: 19056247]
30. Meyer-Lindenberg A, Miletich RS, Kohn PD, Esposito G, Carson RE, Quarantelli M, et al. (2002): Reduced prefrontal activity predicts exaggerated striatal dopaminergic function in schizophrenia. Nat Neurosci. 5:267–271. [PubMed: 11865311]
31. McGowan S, Lawrence AD, Sales T, Quested D, Grasby P (2004): Presynaptic dopaminergic dysfunction in schizophrenia: a positron emission tomographic [18F]fluorodopa study. Arch Gen Psychiatry. 61:134–142. [PubMed: 14757589]
32. Lindstrom LH, Gefvert O, Hagberg G, Lundberg T, Bergstrom M, Hartvig P, et al. (1999): Increased dopamine synthesis rate in medial prefrontal cortex and striatum in schizophrenia indicated by L-(beta-11C) DOPA and PET. Biological psychiatry. 46:681–688. [PubMed: 10472420]
33. Kumakura Y, Cumming P, Vernaleken I, Buchholz HG, Siessmeier T, Heinz A, et al. (2007): Elevated [18F]fluorodopamine turnover in brain of patients with schizophrenia: an [18F]fluorodopa/positron emission tomography study. J Neurosci. 27:8080–8087. [PubMed: 17652599]
34. Howes OD, Kapur S (2009): The dopamine hypothesis of schizophrenia: version III--the final common pathway. Schizophr Bull. 35:549–562. [PubMed: 19325164]
35. Hietala J, Syvalahti E, Vuorio K, Rakkolainen V, Bergman J, Haaparanta M, et al. (1995): Presynaptic dopamine function in striatum of neuroleptic-naive schizophrenic patients. Lancet. 346:1130–1131. [PubMed: 7475604]
36. Insel TR (2010): Rethinking schizophrenia. Nature. 468:187–193. [PubMed: 21068826]
37. Catts VS, Fung SJ, Long LE, Joshi D, Vercammen A, Allen KM, et al. (2013): Rethinking schizophrenia in the context of normal neurodevelopment. Front Cell Neurosci. 7:60. [PubMed: 23720610]
38. Seidman LJ, Cherkerzian S, Goldstein JM, Agnew-Blais J, Tsuang MT, Buka SL (2013): Neuropsychological performance and family history in children at age 7 who develop adult schizophrenia or bipolar psychosis in the New England Family Studies. Psychol Med. 43:119–131. [PubMed: 22575089]
39. Cannon M, Caspi A, Moffitt TE, Harrington H, Taylor A, Murray RM, et al. (2002): Evidence for early-childhood, pan-developmental impairment specific to schizophreniform disorder: results from a longitudinal birth cohort. Arch Gen Psychiatry. 59:449–456. [PubMed: 11982449]
40. Sesack SR, Carr DB (2002): Selective prefrontal cortex inputs to dopamine cells: implications for schizophrenia. Physiol Behav. 77:513–517. [PubMed: 12526992]
41. Weinberger DR (1987): Implications of normal brain development for the pathogenesis of schizophrenia. Arch Gen Psychiatry. 44:660–669. [PubMed: 3606332]
42. Vlasova RM, Iosif AM, Ryan AM, Funk LH, Murai T, Chen S, et al. (2021): Maternal Immune Activation during Pregnancy Alters Postnatal Brain Growth and Cognitive Development in Nonhuman Primate Offspring. J Neurosci. 41:9971–9987. [PubMed: 34607967]
43. Kentner AC, Bilbo SD, Brown AS, Hsiao EY, McAllister AK, Meyer U, et al. (2018): Maternal immune activation: reporting guidelines to improve the rigor, reproducibility, and transparency of the model. Neuropsychopharmacology.
44. Rose SA, Feldman JF, Jankowski JJ (2003): Infant visual recognition memory: independent contributions of speed and attention. Dev Psychol. 39:563–571. [PubMed: 12760523]
45. Weir RK, Forghany R, Smith SE, Patterson PH, McAllister AK, Schumann CM, et al. (2015): Preliminary evidence of neuropathology in nonhuman primates prenatally exposed to maternal immune activation. Brain, behavior, and immunity. 48:139–146. [PubMed: 25816799]

46. Cherel M, Budin F, Prastawa M, Gerig G, Lee K, Buss C, et al. (2015): Automatic Tissue Segmentation of Neonate Brain MR Images with Subject-specific Atlases. Proceedings of SPIE--the International Society for Optical Engineering. 9413.
47. Wang J, Vachet C, Rumple A, Gouttard S, Ouziel C, Perrot E, et al. (2014): Multi-atlas segmentation of subcortical brain structures via the AutoSeg software pipeline. Frontiers in neuroinformatics. 8:7. [PubMed: 24567717]
48. Chan GL, Doudet DJ, Dobko T, Hewitt KA, Schofield P, Pate BD, et al. (1995): Routes of administration and effect of carbidopa pretreatment on 6-[18F]fluoro-L-dopa/PET scans in non-human primates. Life Sci. 56:1759–1766. [PubMed: 7739350]
49. Doudet DJ, Chan GL, Jivan S, DeJesus OT, McGeer EG, English C, et al. (1999): Evaluation of dopaminergic presynaptic integrity: 6-[18F]fluoro-L-dopa versus 6-[18F]fluoro-L-m-tyrosine. J Cereb Blood Flow Metab. 19:278–287. [PubMed: 10078880]
50. Eberling JL, Roberts JA, Taylor SE, VanBrocklin HF, O'Neil JP, Nordahl TE (2002): No effect of age and estrogen on aromatic L- amino acid decarboxylase activity in rhesus monkey brain. Neurobiol Aging. 23:479–483. [PubMed: 11959410]
51. Melega WP, Hoffman JM, Luxen A, Nissenson CH, Phelps ME, Barrio JR (1990): The effects of carbidopa on the metabolism of 6-[18F]fluoro-L-dopa in rats, monkeys and humans. Life Sci. 47:149–157. [PubMed: 2117691]
52. Zwickey RE, Peck HM, Bagdon WJ, Bokelman DL, Brown WR, Hite M, et al. (1974): Preclinical toxicological studies of carbidopa and combinations of carbidopa and levodopa. Toxicol Appl Pharmacol. 29:181–195. [PubMed: 4283683]
53. Patlak CS, Blasberg RG (1985): Graphical evaluation of blood-to-brain transfer constants from multiple-time uptake data. Generalizations. J Cereb Blood Flow Metab. 5:584–590. [PubMed: 4055928]
54. Sossi V, Holden JE, de la Fuente-Fernandez R, Ruth TJ, Stoessl AJ (2003): Effect of dopamine loss and the metabolite 3-O-methyl-[18F]fluoro-dopa on the relation between the 18F-fluorodopa tissue input uptake rate constant Kocc and the [18F]fluorodopa plasma input uptake rate constant Ki. J Cereb Blood Flow Metab. 23:301–309. [PubMed: 12621305]
55. Jordan S, Eberling JL, Bankiewicz KS, Rosenberg D, Coxson PG, VanBrocklin HF, et al. (1997): 6-[18F]fluoro-L-m-tyrosine: metabolism, positron emission tomography kinetics, and 1-methyl-4-phenyl-1,2,3,6-tetrahydropyridine lesions in primates. Brain Res. 750:264–276. [PubMed: 9098552]
56. Keramida G, Hunter J, Peters AM (2016): Hepatic glucose utilization in hepatic steatosis and obesity. Biosci Rep. 36.
57. Laird NM, Ware JH (1982): Random-effects models for longitudinal data. Biometrics. 38:963–974. [PubMed: 7168798]
58. Cohen J (1988): Statistical power analysis for the behavioral sciences. 2 ed. Hillsdale, NJ: L. Erlbaum Associates.
59. Lee MD, Wagenmakers EJ (2014): Bayesian cognitive modeling: A practical course. Cambridge University Press.
60. Goldman-Rakic PS, Brown RM (1982): Postnatal development of monoamine content and synthesis in the cerebral cortex of rhesus monkeys. Brain Res. 256:339–349. [PubMed: 7104766]
61. Irwin I, DeLanney LE, McNeill T, Chan P, Forno LS, Murphy GM Jr., et al. (1994): Aging and the nigrostriatal dopamine system: a non-human primate study. Neurodegeneration. 3:251–265. [PubMed: 7531106]
62. Bernstein IS, Ruehlmann TE, Judge PG, Lindquist T, Weed JL (1991): Testosterone changes during the period of adolescence in male rhesus monkeys (Macaca mulatta). Am J Primatol. 24:29–38. [PubMed: 31952393]
63. Herman RA, Zehr JL, Wallen K (2006): Prenatal androgen blockade accelerates pubertal development in male rhesus monkeys. Psychoneuroendocrinology. 31:118–130. [PubMed: 16112492]
64. Badawi RD, Shi H, Hu P, Chen S, Xu T, Price PM, et al. (2019): First Human Imaging Studies with the EXPLORER Total-Body PET Scanner. J Nucl Med. 60:299–303. [PubMed: 30733314]

65. Horga G, Wengler K, Cassidy CM (2021): Neuromelanin-Sensitive Magnetic Resonance Imaging as a Proxy Marker for Catecholamine Function in Psychiatry. JAMA Psychiatry. 78:788–789. [PubMed: 34009285]
66. McCutcheon R, Beck K, Jauhar S, Howes OD (2018): Defining the Locus of Dopaminergic Dysfunction in Schizophrenia: A Meta-analysis and Test of the Mesolimbic Hypothesis. Schizophr Bull. 44:1301–1311. [PubMed: 29301039]
67. McCutcheon RA, Abi-Dargham A, Howes OD (2019): Schizophrenia, Dopamine and the Striatum: From Biology to Symptoms. Trends Neurosci. 42:205–220. [PubMed: 30621912]
68. D'Ambrosio E, Jauhar S, Kim S, Veronese M, Rogdaki M, Pepper F, et al. (2021): The relationship between grey matter volume and striatal dopamine function in psychosis: a multimodal (18)F-DOPA PET and voxel-based morphometry study. Mol Psychiatry. 26:1332–1345. [PubMed: 31690805]
69. Smucny J, Dienel SJ, Lewis DA, Carter CS (2022): Mechanisms underlying dorsolateral prefrontal cortex contributions to cognitive dysfunction in schizophrenia. Neuropsychopharmacology. 47:292–308. [PubMed: 34285373]
70. Gilbert MH, Baker KC (2011): Social buffering in adult male rhesus macaques (Macaca mulatta): Effects of stressful events in single vs. pair housing. J Med Primatol. 40:71–78. [PubMed: 21371035]
71. Hennessy MB, Chun K, Capitanio JP (2017): Depressive-like behavior, its sensitization, social buffering, and altered cytokine responses in rhesus macaques moved from outdoor social groups to indoor housing. Soc Neurosci. 12:65–75. [PubMed: 26801639]
72. Hostinar CE, Sullivan RM, Gunnar MR (2014): Psychobiological mechanisms underlying the social buffering of the hypothalamic-pituitary-adrenocortical axis: a review of animal models and human studies across development. Psychol Bull. 140:256–282. [PubMed: 23607429]
73. Gunnar MR (2017): Social Buffering of Stress in Development: A Career Perspective. Perspect Psychol Sci. 12:355–373. [PubMed: 28544861]
74. Beck K, Studerus E, Andreou C, Egloff L, Leanza L, Simon AE, et al. (2019): Clinical and functional ultra-long-term outcome of patients with a clinical high risk (CHR) for psychosis. Eur Psychiatry. 62:30–37. [PubMed: 31514058]
75. O'Brien MP, Gordon JL, Bearden CE, Lopez SR, Kopelowicz A, Cannon TD (2006): Positive family environment predicts improvement in symptoms and social functioning among adolescents at imminent risk for onset of psychosis. Schizophr Res. 81:269–275. [PubMed: 16309893]
76. Schlosser DA, Zinberg JL, Loewy RL, Casey-Cannon S, O'Brien MP, Bearden CE, et al. (2010): Predicting the longitudinal effects of the family environment on prodromal symptoms and functioning in patients at-risk for psychosis. Schizophr Res. 118:69–75. [PubMed: 20171848]
77. Koutra K, Triliva S, Roumeliotaki T, Basta M, Simos P, Lionis C, et al. (2015): Impaired family functioning in psychosis and its relevance to relapse: a two-year follow-up study. Compr Psychiatry. 62:1–12. [PubMed: 26343461]
78. Giovanoli S, Engler H, Engler A, Richetto J, Feldon J, Riva MA, et al. (2016): Preventive effects of minocycline in a neurodevelopmental two-hit model with relevance to schizophrenia. Transl Psychiatry. 6:e772. [PubMed: 27045842]
79. Giovanoli S, Engler H, Engler A, Richetto J, Voget M, Willi R, et al. (2013): Stress in puberty unmasks latent neuropathological consequences of prenatal immune activation in mice. Science. 339:1095–1099. [PubMed: 23449593]
80. Astle DE, Barnes JJ, Baker K, Colclough GL, Woolrich MW (2015): Cognitive training enhances intrinsic brain connectivity in childhood. J Neurosci. 35:6277–6283. [PubMed: 25904781]
81. Park AT, Tooley UA, Leonard JA, Boroshok AL, McDermott CL, Tisdall MD, et al. (2021): Early childhood stress is associated with blunted development of ventral tegmental area functional connectivity. Dev Cogn Neurosci. 47:100909. [PubMed: 33395612]

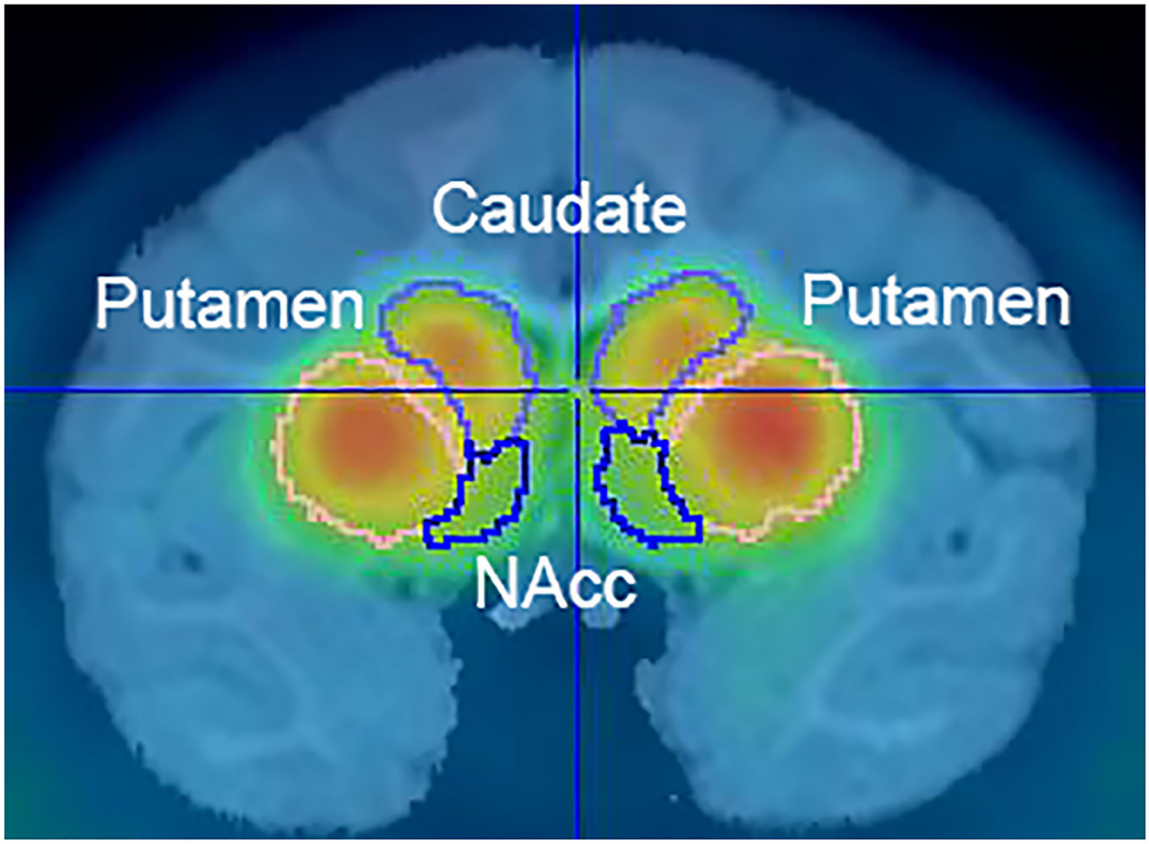

Figure 1.
Representative PET scan showing dopamine synthesis capacity within outlined caudate, putamen, and NAcc regions of interest. Scan is from a 26-month macaque in the maternal immune activation (MIA) group.

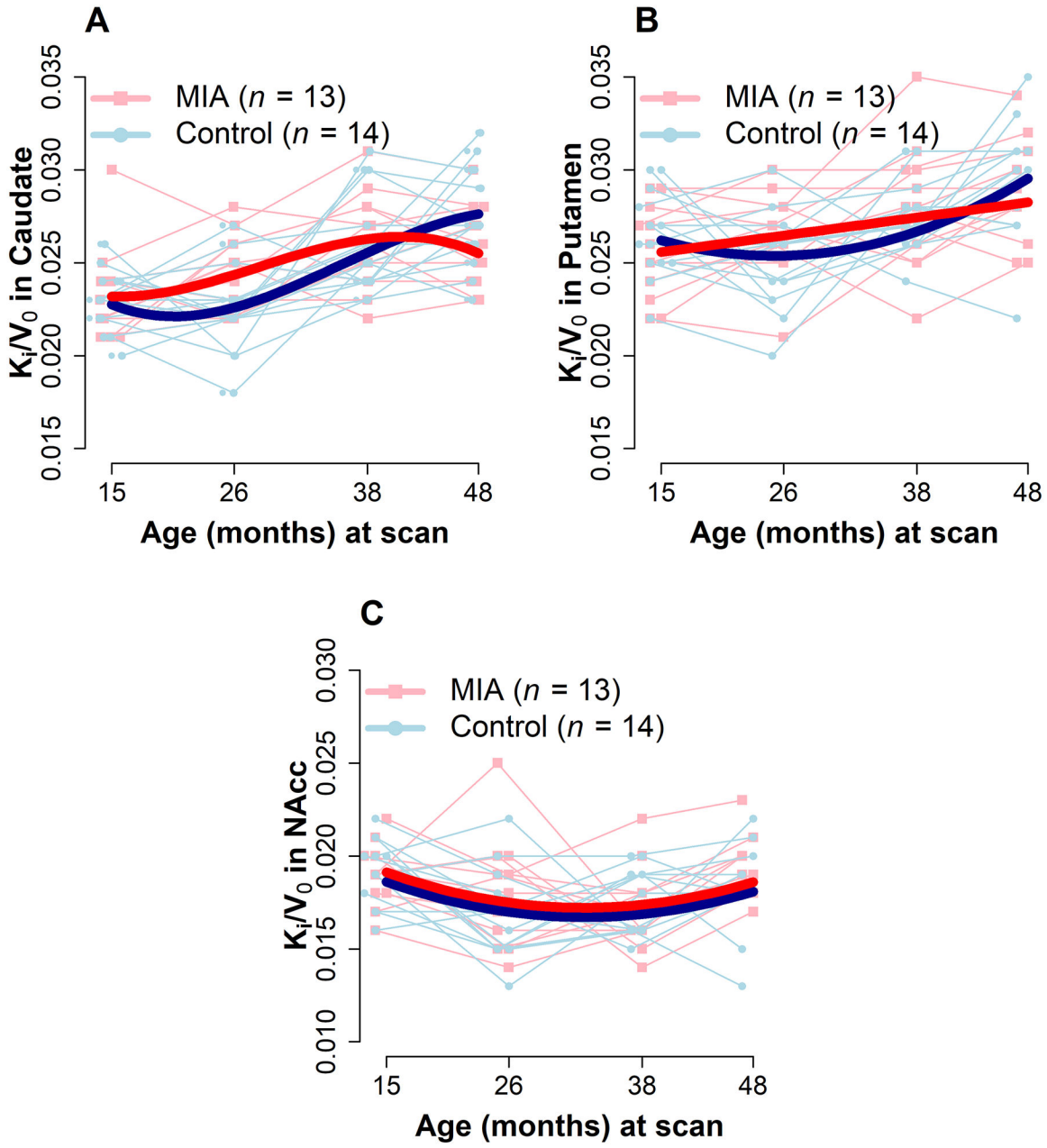

Figure 2.

Trajectories of [^{18}F]FMT PET signal (K_i/V_0) in the caudate (a), putamen (b), and nucleus accumbens (c; NAcc) for maternal immune activation (MIA) and control offspring from 15 through 48 months. The light lines represent observed individual trajectories and dark lines represent the average estimated trajectory for the two groups from the final models. For caudate, the signal (K_i/V_0) was significantly higher in the MIA group at the 26-month timepoint relative to the control group. n=12 at 48 months of age for the MIA group as one animal was euthanized prior to scanning.

Table 1.

Summary data from 15 to 48 months for MIA-exposed and control offspring.

	15 Months		26 Months		38 Months		48 Months	
	MIA (*n* = 13)	**Control (*n* = 14)**	**MIA (*n* = 13)**	**Control (*n* = 14)**	**MIA (*n* = 13)**	**Control (*n* = 14)**	**MIA (*n* = 12)[a]**	**Control (*n* = 14)**
Age (days) at scan, *mean* (*SD*) [*Range*]								
	446 (22)	445 (25)	790 (5)	791 (3)	1157 (4)	1158 (6)	1458 (11)	1453 (8)
	[425–493]	[423–487]	[775–794]	[784–797]	[1146–1167]	[1149–1168]	[1441–1476]	[1443–1467]
Weight (kg) at scan, *mean* (*SD*) [*Range*]								
	2.6 (0.3)	2.6 (0.5)	3.9 (0.6)	3.9 (0.5)	6.0 (1.0)	5.8 (1.0)	7.7 (1.1)	7.6 (1.3)
	[2.0–3.4]	[1.8–3.5]	[3.0–5.0]	[2.9–4.9]	[4.7–7.4]	[4.5–7.6]	[6.1–9.3]	[5.6–9.4]
Dose/weight (mCi/kg) at scan, *mean* (*SD*) [*Range*]								
	0.51 (0.03)	0.54 (0.03)	0.49 (0.05)	0.49 (0.04)	0.50 (0.02)	0.51 (0.05)	0.49 (0.04)	0.49 (0.03)
	[0.43–0.56]	[0.50–0.61]	[0.41–0.54]	[0.42–0.57]	[0.47–0.52]	[0.39–0.60]	[0.37–0.53]	[0.44–0.53]
PET K_i/V_0 *mean* (*SD*)								
Caudate	0.023 (0.002)	0.023 (0.002)	0.025 (0.002)	0.022 (0.002)	0.026 (0.003)	0.026 (0.003)	0.026 (0.002)	0.027 (0.003)
Putamen	0.026 (0.002)	0.026 (0.002)	0.026 (0.002)	0.025 (0.002)	0.028 (0.003)	0.027 (0.002)	0.029 (0.003)	0.029 (0.003)
NAcc	0.019 (0.002)	0.019 (0.002)	0.018 (0.003)	0.017 (0.002)	0.017 (0.002)	0.017 (0.002)	0.019 (0.002)	0.018 (0.002)

Abbreviations: MIA = maternal immune activation, NAcc = nucleus accumbens, SD = standard deviation.

[a]An animal from the MIA-exposed group was euthanized at 42 months of age due to an unrelated health condition and thus did not contribute data at 48 months.

Table 2.

Parameter estimates from the linear mixed-effects models examining trajectories of K_i/V_0 (in 10^{-3}) from 15 to 48 months in MIA-exposed and control offspring.

		Caudate		Putamen		NAcc	
Model Term	**Description**	**Estimate (*SE*)**	***P***	**Estimate (*SE*)**	***P***	**Estimate (SE)**	***P***
Intercept	Baseline (15 months) level in control	22.755 (0.505)	<0.001	26.199 (0.670)	<0.001	18.617 (0.422)	<0.001
Group	Difference (in 10^{-3}) MIA vs. control at 15 months	0.433 (0.727)	0.556	−0.625 (0.966)	0.519	0.507 (0.412)	0.225
Age (linear)	Effect of age (centered at 15 months) in control	−0.242 (0.128)	0.062	−0.163 (0.083)	0.053	−0.214 (0.054)	<0.001
Age^2	$(Age-15)^2$	0.025 (0.010)	0.011	0.008 (0.002)	0.001	0.006 (0.002)	<0.001
Age^3	$(Age-15)^3$	−0.0004 (0.0002)	0.038	-	-	-	-
Group*age (linear)	Difference in linear age effect between MIA and control	0.220 (0.107)	0.044	0.244 (0.120)	0.044	-	-
Group*age^2	Difference in group difference when $(age-15)^2$ increases by one month	−0.009 (0.003)	0.008	−0.008 (0.003)	0.034	-	-

Adjusted difference in K_i/V_0 (in 10^{-3}) MIA vs. control at different ages

	Caudate				Putamen			
	Cohen's D	**Estimate (*SE*)**	***P***	**Bayes Factor**	**Cohen's D**	**Estimate (*SE*)**	***P***	**Bayes Factor**
15 Months	0.21	0.43 (0.73)	0.556	0.86	−0.28	−0.63 (0.97)	0.519	1.11
26 Months	**0.84**	**1.79 (0.71)**	**0.015**	**19.11**	0.49	1.15 (0.86)	0.185	1.42
38 Months	0.32	0.87 (0.79)	0.280	0.90	0.38	1.01 (0.84)	0.231	2.23
48 Months	−0.73	−1.81 (1.02)	0.084	2.59	−0.25	−0.76 (1.02)	0.461	1.28

Abbreviations: NAcc = nucleus accumbens, MIA = maternal immune activation, SE = standard error, SD = standard deviation.

Separate mixed-effects linear models were fitted to 13 MIA (1 missing data at 48 months) and 14 control animals in each region. Initial models included fixed effects for group, age at scan (in months, centered at 15 months, with linear, squared, and cubic terms), interactions between group and age (linear, squared, and cubic), and within-animal covariance structures to account for repeated measures over time. Within-animal covariance structures were modeled by spatial exponential correlation for the putamen and NAcc. For caudate, within-animal covariance was modeled by including a random intercept and a random slope of age. Because of centering, the intercept can be interpreted as the predicted K_i/V_0 (in 10^{-3}) at 15 months for a control animal and the difference (in 10^{-3}) MIA vs. control can be interpreted as the average group difference at 15 months of age. Interactions between group and effects of age as well as higher order age effects were removed if non-significant. For the NAcc, the interaction effects were non-significant and therefore not retained in the final model; adjusted age-specific differences vs. control are therefore not reported for this ROI. At each timepoint, effect sizes were calculated using Cohen's D = (MIA mean-Control mean)/SD, where the group differences (MIA mean-Control mean) were estimated based on the fitted linear mixed-effects models and SDs were the pooled standard deviations from MIA and control groups at each timepoint. Bayes factors were calculated to evaluate the strength of the evidence for group differences at each timepoint. Bayes factors between 3 – 10, 10 – 30, and > 30 are interpreted as moderate, strong, and very strong/extreme evidence for the alternative hypothesis, respectively; factors between 1/3 – 1/10, 1/10 – 1/30, and < 1/30 are interpreted as moderate, strong, and very strong/extreme evidence for the null, respectively. A Bayes factor between 1/3 and 3 provides only weak or "anecdotal" evidence (59).